Available online at www.sciencedirect.com
ScienceDirect
Journal of Power Sources 174 (2007) 756–760
JOURNAL OF POWER SOURCES
www.elsevier.com/locate/jpowsour

Short communication

Crystallization of $LiMn_2O_4$ observed with high temperature X-ray diffraction

A. Ogata, T. Shimizu, S. Komaba *

Department of Applied Chemistry, Faculty of Science, Tokyo University of Science, 1-3 Kagurazaka, Shinjuku, Tokyo 162-8601, Japan

Available online 28 June 2007

Abstract

We investigated the formation of $LiMn_2O_4$ phases by calcinating a stoichiometric mixture of Li_2CO_3 and various manganese compounds with high temperature X-ray diffraction (HT-XRD) technique to understand the influence of starting materials on the electrochemical performance. XRD measurements were carried out during heating processes from room temperature to 700 °C. In case of Li_2CO_3/electrolytic manganese dioxide and $Li_2CO_3/MnCO_3$ mixtures used as starting materials, $Li_{0.33}MnO_2$ phase and low crystalline phase, respectively, appeared as intermediate products during heating process followed by the crystallization into the spinel. HT-XRD observation confirmed that the $LiMn_2O_4$ phase was directly formed from starting Li_2CO_3/Mn_2O_3 and Li_2CO_3/Mn_3O_4 mixtures. The reactivity of the mixture, meant by the lower reaction temperature between Li and Mn compounds and the faster evolution of Li–Mn–O phase, depended on manganese compounds. The purity and stoichiometry of spinel type $LiMn_2O_4$ was not achieved only by the higher reactivity. From these results, the dependence of reversible capacities and cycleability of synthesized $LiMn_2O_4$s on the formation process which varied with the starting materials was discussed.

Keywords: $LiMn_2O_4$; High temperature XRD; Crystallization; Lithium-ion battery

1. Introduction

As the most promising cathode materials for Li ion batteries, many research works on Li–Mn–O compounds such as spinel type $LiMn_2O_4$ were reported in the past decade. The stoichiometric and non-stoichiometric spinel can be obtained over a wide compositional range including the Li-rich spinel and oxygen-rich or -deficient spinel [1–4]. Up to now the syntheses of the spinels are achieved by various methods such as solid-state reaction [1–13], melt-impregnation [14,15], emulsion drying [16,17], sol–gel [18,19], and so on.

Among these synthetic methods, solid-state reaction is commonly used for manufacturing cathodic oxide materials for Li-ion batteries. In case of solid-state reaction, physical and electrochemical performances of synthesized spinels depend on the different synthetic conditions, however, the relation between the synthetic conditions including starting material and electrochemical properties was not completely understood in previous literatures to our knowledge [7,8,11–13]. The stoichiometry, crystallinity, particle size/shape, and surface condition of the spinel were influenced by the selection of starting lithium and manganese compounds even if the same heating conditions. Therefore, we here study the crystallization process of Li–Mn–O spinel from several starting mixtures by measuring diffraction patterns in situ at high temperature, and we discussed the relation between the crystallization process, the resultant crystallinity and electrochemical properties of the spinel cathode.

2. Experimental

$LiMn_2O_4$s were prepared from a mixture of reagent grade Li_2CO_3 and various Mn sources such as electrolytic manganese dioxides (EMD, IC-17), $MnCO_3$, Mn_2O_3 or Mn_3O_4. Inductively coupled plasma atomic emission spectrometry (Hitachi P-4010, Japan) was used to determine the exact Mn and Li contents of these sources prior to use, and a stoichiometric mixture (Li/Mn atomic ratio = 1/2) was ground with planetary ball-milling. $LiMn_2O_4$s were synthesized by calcinations of these mixtures at 700 °C for 12 h in air at 1 °C min^{-1}. High temperature X-ray diffraction (HT-XRD, MultiFlex, SHT-1500 and PTC-30, Rigaku Co. Ltd., Japan) was employed for observation of synthesis process at given temperature. XRD data were col-

* Corresponding author.
E-mail address: komaba@rs.kagu.tus.ac.jp (S. Komaba).

0378-7753/$ – see front matter © 2007 Elsevier B.V. All rights reserved.
doi:10.1016/j.jpowsour.2007.06.150

lected at 25 °C and during heating steps from 100 to 700 °C every 50 °C. After reaching the given temperature by sweeping temperature at 1 °C min^{-1}, it was held at each temperature for 5 min prior to data collection, and then the XRD data were collected for 50 min in the region of 10–90° in 2θ. Thermogravimetric analysis (TG, DTG-60, Shimadzu Co. Ltd., Japan) was performed on the starting materials of Li_2CO_3 and $MnCO_3$, Mn_2O_3, Mn_3O_4 or EMD. These mixtures were placed in Pt crucibles, heated in air up to 700 °C at a rate of 1 °C min^{-1}. For electrochemical measurements, positive electrode mixtures consisted of $LiMn_2O_4$, acetylene black as conductive agent and poly(vinylidene fluoride) as a binder, in a weight ratio of 8:1:1. A lithium foil was used for counter electrode. A battery grade electrolyte used was 1 mol dm^{-3} $LiPF_6$-ethylene carbonate (EC):dimethyl carbonate (DMC) (1:1, v/v). Charge–discharge tests as a positive electrode were carried out between 3.0 and 4.5 V versus Li/Li$^+$ at 20 mA g^{-1} and 25 °C.

3. Results and discussion

Fig. 1(A) shows XRD patterns of synthesized samples from several manganese sources under the same calcination conditions. All peaks in the XRD patterns of the synthesized samples can be indexed as the spinel phase (JCPDS: 35-0782). Because of no diffraction peaks of impurity phases, therefore, we successfully obtained single-phase products of $LiMn_2O_4$ by calcinations at 700 °C from Li_2CO_3 and several manganese sources. The lattice parameters of *a*-axis of these cubic spinels are between 8.239 and 8.248 Å which would correspond to that of stoichiometric spinel.

Fig. 1(B) indicates magnified patterns from 2θ = 80–82°. The peak around 2θ = 81° corresponds to (4 4 4) diffraction line of the spinel. In these XRD patterns, peak splitting due to Cu Kα1 and Kα2 radiation was distinguishable for $LiMn_2O_4$s synthesized from Mn_2O_3 and $MnCO_3$. But in case of EMD and Mn_3O_4, the corresponding peaks are not split clearly due to broadened diffraction peaks. That is, the spinels crystallized from Mn_2O_3 and $MnCO_3$ have higher crystallinity than those from EMD and Mn_3O_4 even under the same calcination conditions. It is clear that the difference of manganese compounds used as starting materials influenced the reactivity with lithium carbonate, resulting in the different crystallinity of spinels.

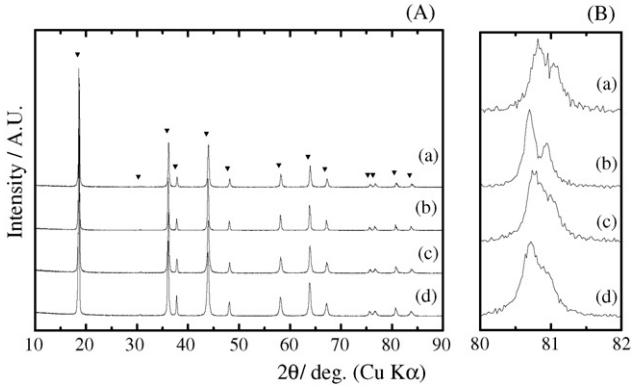

Fig. 1. XRD patterns of various synthesized spinels from Li_2CO_3 and different manganese sources: (a) $MnCO_3$, (b) Mn_2O_3, (c) Mn_3O_4, and (d) EMD. Diffraction angle ranges are (A) 10–90° and (B) 80–82° in 2θ. ▼: Spinel $LiMn_2O_4$.

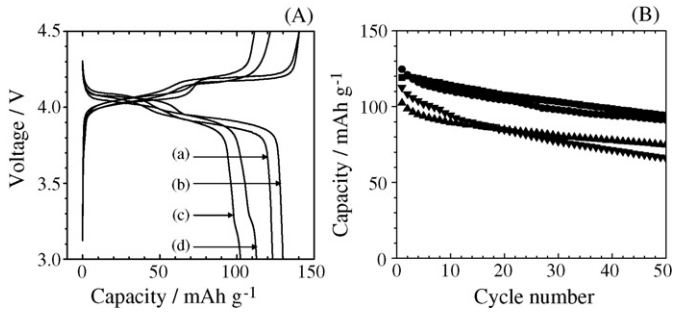

Fig. 2. (A) First charge–discharge curves of four spinels synthesized from (a) $MnCO_3$, (b) Mn_2O_3, (c) Mn_3O_4, and (d) EMD. (B) Discharge capacity vs. cycle number plots of $LiMn_2O_4$s by various manganese sources: (●) Mn_2O_3, (▲) Mn_3O_4, (▼) EMD, (■) $MnCO_3$ as starting materials.

The first charge–discharge curves of spinels from various manganese sources and variation in discharge capacities of these spinels are shown in Fig. 2. In Fig. 2(A), two plateaus which originated from stoichiometric $LiMn_2O_4$ are observed in charge and discharge curves around 4 V. In case of Mn_2O_3 and $MnCO_3$, reversible capacities are 120–130 mAh g^{-1} similarly to previous literature [1,3,14,15]. However, the spinels prepared from EMD and Mn_3O_4 have reversible capacities of about 100 mAh g^{-1}. Their reversible capacities are lower in comparison with those from Mn_2O_3 and $MnCO_3$, additionally, tiny plateaus around 3.2 V are observed owing to the slight oxygen deficiency of spinel as reported previously [3,5]. The oxygen-deficiency of spinels can be avoided by calcinating in oxidizing atmosphere. In Fig. 2(B), the spinels prepared from Mn_2O_3 and $MnCO_3$ maintained relatively high discharge capacities during 50 cycles. Compared with these capacities, the discharge capacities for EMD and Mn_3O_4 were obviously fading and lower. According to previous reports [11–13], it is likely that the reactions of these starting mixtures cause oxygen deficiency due to lower oxygen activity. As mentioned in Fig. 1, the lower crystallinity spinels were obtained from Mn_3O_4 and EMD, further, they have oxygen deficiency as seen in Fig. 2. The electrochemical performance was affected by the crystallinity and oxygen stoichiometry resulting from different starting materials. That is, the electrochemical performances depended on the reactivity of four Mn compounds with Li_2CO_3 that should influence the resultant spinels. In general, the reactivity is improved by higher temperature and/or prolonged calcination time and so on. In order to examine the different reactivity, we did investigate the formation processes from starting mixture to spinels under the same heating conditions with HT-XRD.

Figs. 3–6 show HT-XRD patterns of the starting lithium and manganese mixtures of $MnCO_3$, Mn_2O_3, Mn_3O_4 and EMD, respectively, during heating up to 700 °C. For $MnCO_3$ as manganese source, the diffraction peaks of the starting materials did not change up to 200 °C at all, and then this mixture underwent decomposition reaction to form low crystalline phase at higher temperature around 300 °C. Also TG curve of the mixture showed that the weight loss corresponds to the decomposition reaction. From around 350 °C, broad spinel peaks began

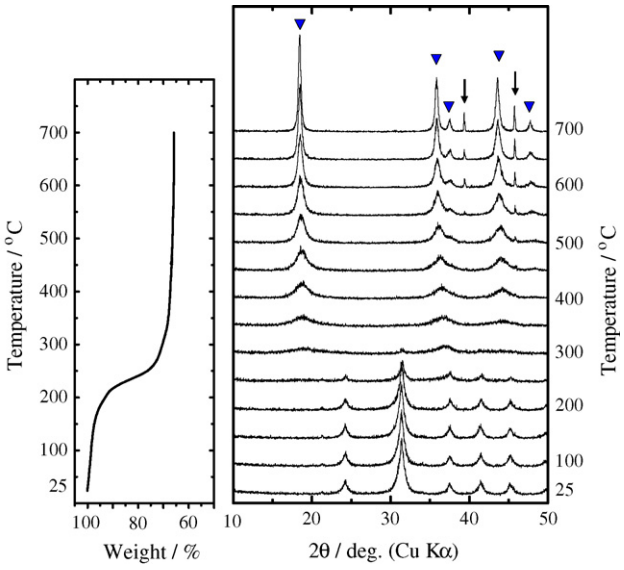

Fig. 3. HT-XRD patterns (right) and TG curve (left) of Li_2CO_3 and $MnCO_3$ as starting materials. ▼: Spinel, ↓: Pt holder.

to appear, and the peaks became sharp about 350–700 °C. The mass of this mixture was almost constant in the temperature range. It is suggested that crystal growth of single $LiMn_2O_4$ phase progressed during heating.

HT-XRD patterns obtained with Mn_2O_3 are shown in Fig. 4. When Mn_2O_3 is used as a manganese source, the phase evolution during calcinations differs from that of $MnCO_3$. The initial diffraction peaks of the mixture of Li_2CO_3 and Mn_2O_3 are observed with maintenance of their sharpness up to 350 °C, and diffraction intensity of $LiMn_2O_4$ become gradually higher up to 700 °C, simultaneously, intensity of Mn_2O_3 peaks decreased while maintaining the similar narrow peak width of not only Mn_2O_3 but $LiMn_2O_4$. When the temperature reached at 700 °C, the small peaks of Mn_2O_3 around 33° in 2θ still remained though the main phase was $LiMn_2O_4$. The Mn_2O_3 completely disappeared during annealing for 12 h at 700 °C. From TG and HT-XRD, the formation of $LiMn_2O_4$ took place at temperature range from about 300 to 500 °C. It shows that the weight loss of decomposition reaction of Li_2CO_3 at temperature from 300 to 380 °C, and mass increase involved oxidation of Mn compound between 380 and 450 °C. We found that the reaction between Li_2CO_3 and Mn_2O_3 led to gradual formation of $LiMn_2O_4$ but direct formation because of no intermediate phases. From these results, it seems that the formation of $LiMn_2O_4$ occurred with lithium penetration into Mn_2O_3, so that particle size of $LiMn_2O_4$ was similar to that of Mn_2O_3 as confirmed by SEM. The temperature where the peaks of starting material begin to be weakened is higher than that of $MnCO_3$. This means that the reactivity of Li_2CO_3 and Mn_2O_3 is lower than that of Li_2CO_3 and $MnCO_3$.

Fig. 5 shows HT-XRD patterns obtained from a mixture of Li_2CO_3 and Mn_3O_4. HT-XRD patterns exhibit reacting Mn_3O_4

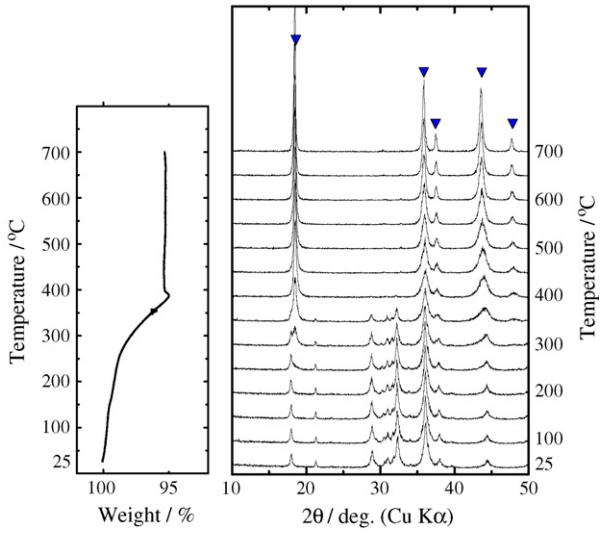

Fig. 5. HT-XRD patterns (right) and TG curve (left) of Li_2CO_3 and Mn_3O_4 as starting material. ▼: Spinel.

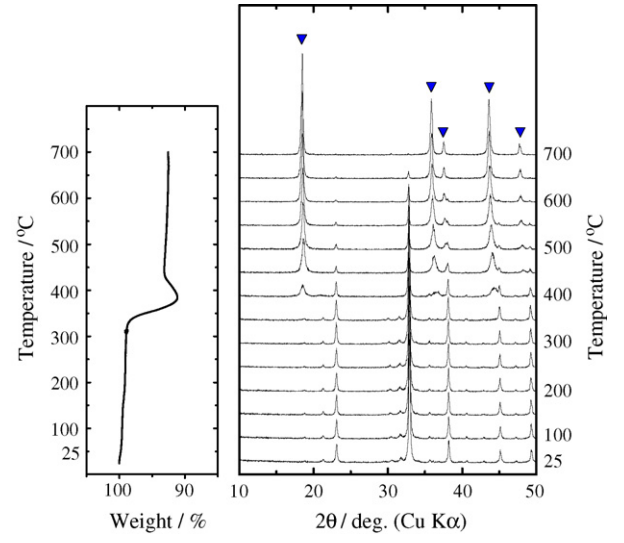

Fig. 4. HT-XRD patterns (right) and TG curve (left) of Li_2CO_3 and Mn_2O_3 as starting material. ▼: Spinel.

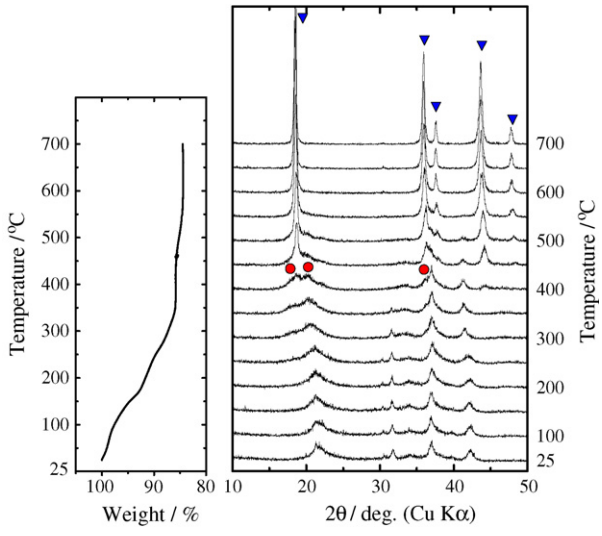

Fig. 6. HT-XRD patterns (right) and TG curve (left) of Li_2CO_3 and EMD as starting material. ▼: Spinel, ●: $Li_{0.33}MnO_2$.

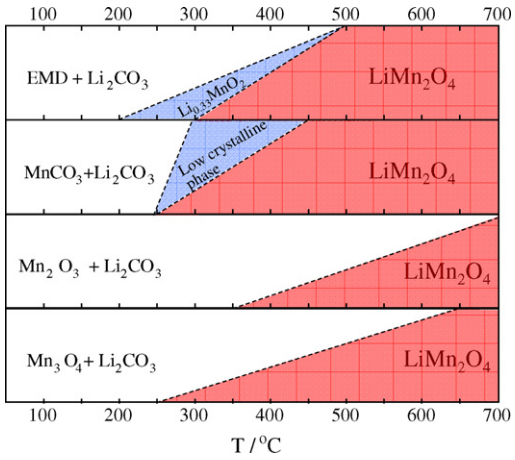

Fig. 7. Phase evolutions from each starting material to $LiMn_2O_4$ vs. temperature during heating process.

with Li_2CO_3 from low temperature of 250 °C. The mixture was transformed into $LiMn_2O_4$ between 250 and 650 °C, then Mn_3O_4 peaks disappeared in the patterns, and $LiMn_2O_4$ single phase appeared at 650 °C and higher temperature. It is found that Mn_3O_4 with Li salt reacts via no intermediate products to produce $LiMn_2O_4$ directly similarly to that of Mn_2O_3. Moreover the weight of starting material gradually decreased up to 380 °C and then the mass slightly increased in TG curve. The trend is similar to the case of Mn_2O_3. Up to 380 °C, weight loss of decomposition reaction of Li_2CO_3 and mass increase for oxidation of Mn after 380 °C. The reaction between Li_2CO_3 and Mn_3O_4 begins at lower temperature of 250 °C than the temperature from Mn_2O_3, 350 °C (Fig. 4). From these results, Mn_3O_4 possesses higher reactivity with Li_2CO_3 than that of Mn_2O_3, though the crystallinity of $LiMn_2O_4$ from Mn_3O_4 was lower than that of Mn_2O_3.

In case of EMD as shown in Fig. 6, diffraction peaks of starting materials hardly changed until 200 °C, followed by the formation of $Li_{0.33}MnO_2$ [20–22] as an intermediate phase from 250 °C, suggesting the highest reactivity with Li_2CO_3 among four Mn compounds. Between 350 and 500 °C two phases of $Li_{0.33}MnO_2$ and $LiMn_2O_4$ are coexisted. A $Li_{0.33}MnO_2$ phase was observed only for EMD. At >550 °C, $LiMn_2O_4$ single phase appeared, and the diffraction peaks of the spinel are gradually intensified with elevating temperature. Consequently, lithium carbonate reacted with EMD producing $Li_{0.33}MnO_2$ above 250 °C thereafter $LiMn_2O_4$ at higher temperature than 550 °C. It seems that this mixture gradually decreased in mass value from TG curve. Up to about 200 °C, weight loss is probably due to release of adsorbed water in EMD and it was followed by the decomposition reaction of Li_2CO_3 after 200 °C. We compared the HT-XRD for powder and pellet of a mixture of Li_2CO_3 and Mn_2O_3. As a result, pellet was suitable to accelerate the crystallization of $LiMn_2O_4$ because intimate contact between Li_2CO_3 and Mn_2O_3 in pellet is adequate for solid-state reaction.

Fig. 7 summarizes the phase evolutions from each starting material to $LiMn_2O_4$ versus temperature during heating. Note that the reaction temperature and intermediate phase formation during heating processes depended on the starting materials. In case of EMD, high reactivity was achieved because reaction occurred at the lowest temperature among them; however, oxygen deficiency spinel was formed via intermediate phase. Also, the similar oxygen deficiency was observed in case of Mn_3O_4. Although reactivity is high for Li_2CO_3/EMD and Li_2CO_3/Mn_3O_4, the electrochemical performances were not satisfactory because of lower crystalline and non-stoichiometry. On the other hand, the Mn_2O_3 showed low reactivity, but we obtained high crystallinity and stoichiometric spinel phase demonstrating the sufficient battery performance. From the above observation, we concluded that the electrochemical characteristics were influenced by not only reactivity of starting materials but crystallization process that determine crystallinity and stoichiometry. Direct spinel formation and higher reactivity are not always beneficial to solid-state reaction to from spinel type $LiMn_2O_4$. That is, synthesis of composite oxides, such as $LiMn_2O_4$, $LiNi_{1/2}Mn_{1/2}O_2$, and so on, required understanding the calcination condition and its formation process to obtain their original electrochemical ability experimentally.

4. Conclusion

The spinel type $LiMn_2O_4$s synthesized from Li_2CO_3 and various manganese materials with calcination conditions at 700 °C for 12 h were single-phase products. Their crystallization process was observed in situ by means of HT-XRD. In spite of the similar final spinel, the crystallization route was dependent on the starting materials. It was found that not only the reactivity but also the intermediate reaction route important to obtain highly crystalline and stoichiometric $LiMn_2O_4$. The $LiMn_2O_4$ synthesized from Mn_2O_3 and $MnCO_3$ had higher crystallinity and the deficiency free resulting in the sufficient electrochemical performance compared to the other manganese sources.

Acknowledgments

This study was financially supported by the Iwatani Naoji Foundation's Research Grant and Yazaki Memorial Foundation for Science and Technology.

References

[1] R.J. Gummow, A. de Kock, M.M. Thackeray, Solid State Ionics 69 (1994) 59.
[2] C. Masquelier, M. Tabuchi, K. Ado, R. Kanno, Y. Kobayashi, Y. Maki, O. Nakamura, J.B. Goodenough, J. Solid State Chem. 123 (1996) 255.
[3] Y. Xia, T. Sakai, T. Fujieda, X.Q. Yang, X. Sun, Z.F. Ma, J. McBreen, M. Yoshio, J. Electrochem. Soc. 148 (2001) A723.
[4] J.M. Paulsen, J.R. Dahn, Chem. Mater. 11 (1999) 3065.
[5] Y. Gao, J.R. Dahn, J. Electrochem. Soc. 143 (1996) 100.
[6] T. Ohzuku, M. Kitagawa, T. Hirai, J. Electrochem. Soc. 137 (1990) 769.
[7] X.H. Hu, X.P. Ai, H.X. Yang, Sh.X. Li, J. Power Sources 74 (1998) 240.
[8] Y. Sun, Z. Wang, L. Chen, X. Huang, J. Electrochem. Soc. 150 (2003) A1294.
[9] Y. Xia, N. Kumada, M. Yoshio, J. Power Sources 90 (2000) 135.
[10] R. Kanno, M. Yonemura, T. Kohigashi, Y. Kawamoto, M. Tabuchi, T. Kamiyama, J. Power Sources 97–98 (2001) 423.
[11] V. Berbenni, A. Marini, J. Anal. Appl. Pyrol. 62 (2002) 45.
[12] V. Berbenni, A. Marini, J. Anal. Appl. Pyrol. 64 (2002) 43.
[13] V. Berbenni, A. Marini, J. Anal. Appl. Pyrol. 70 (2003) 437.

[14] Y. Xia, Y. Zhou, M. Yoshio, J. Electrochem. Soc. 144 (1997) 2593.
[15] Y. Xia, M. Yoahio, J. Electrochem. Soc. 144 (1997) 4186.
[16] S.-T. Myung, H.-T. Chung, S. Komaba, N. Kumagai, H.-B. Gu, J. Power Sources 90 (2000) 103.
[17] S.-T. Myung, S. Komaba, N. Kumagai, J. Electrochem. Soc. 148 (2001) A482.
[18] S. Choi, A. Manthiram, J. Electrochem. Soc. 147 (2000) 1623.
[19] Y.-K. Sun, I.-H. Oh, K.Y. Kim, Ind. Eng. Chem. Res. 36 (1997) 4839–4846.
[20] N. Kumagai, T. Saito, S. Komaba, J. Appl. Electrochem. 30 (2000) 159.
[21] M. Yoshio, H. Nakamura, Y. Xia, Electrochem. Acta 45 (1999) 273.
[22] E. Levi, E. Zinigrad, H. Teller, M.D. Levi, D. Aurbach, J. Electrochem. Soc. 145 (1998) 3440.